Transgenic Research (2005) 14:385–395
DOI 10.1007/s11248-005-0439-0
© Springer 2005

Production of dextran in transgenic potato plants

Géraldine A. Kok-Jacon[1,‡], Jean-Paul Vincken[1], Luc C.J.M. Suurs[1], Denong Wang[2,3], Shaoyi Liu[3] & Richard G.F. Visser[1,*]

[1]*Graduate School Experimental Plant Sciences, Laboratory of Plant Breeding, Wageningen University, P.O. Box 386, 6700 AJ Wageningen, The Netherlands*

[2]*Departments of Genetics, Neurology and Neurological Sciences, Stanford University School of Medicine, Beckman Center B006, Stanford, CA 94305-5318, USA*

[3]*Functional Genomics Division, Columbia Genome Center, College of Physicians and Surgeons, Columbia University, 1150 St. Nicholas Avenue, New York, NY 10032, USA*

Received 17 October 2004; accepted 4 January 2005

Key words: dextran, glucansucrase, granule morphology, transgenic potato

Abstract

The production of dextran in potato tubers and its effect on starch biosynthesis were investigated. The mature dextransucrase (*DsrS*) gene from *Leuconostoc mesenteroides* was fused to the chloroplastic ferredoxin signal peptide (FD) enabling amyloplast entry, which was driven by the highly tuber-expressed patatin promoter. After transformation of two potato genotypes (cv. Kardal and the amylose-free (*amf*) mutant), dextrans were detected by enzyme-linked immunosorbent assay (ELISA) in tuber juices of Kardal and *amf* transformants. The dextran concentration appeared two times higher in the Kardal (about 1.7 mg/g FW) than in the *amf* transformants. No dextran was detected by ELISA inside the starch granule. Interestingly, starch granule morphology was affected, which might be explained by the accumulation of dextran in tuber juices. In spite of that, no significant changes of the physicochemical properties of the starches were detected. Furthermore, we have observed no clear changes in chain length distributions, despite the known high acceptor efficiency of DSRS.

Introduction

The use of plants for the production of novel polymers is an emerging technology of great interest (Kok-Jacon et al., 2003). Studies based on the accumulation of fructan (Gerrits, 2000) and silk (Scheller et al., 2001) in potato have indicated that plants can be used as bioreactors for the production of novel polymers. Furthermore, modification of native polymers such as starch might be possible. For instance, attachment of fructosyl residues to starch was also investigated by expressing a sucrose-converting enzyme, the SACB levansucrase, in potato amyloplasts. Attachment of fructan to starch was demonstrated in small amounts in *in vitro* experiments, and it was hypothesized that this might also occur *in planta* (Gerrits, 2000).

Biosynthesis of dextrans is mediated by *Lactobacillus*, *Leuconostoc*, and *Streptococcus* bacteria in the presence of sucrose. Dextrans are extracellular α-glucans composed of α-(1→6)-linked glucosyl residues in the main chain, and branched by variable proportions of α-(1→2), α-(1→3) or α-(1→4) linked glucose, depending on their origin (Jeanes et al., 1954; Sidebotham, 1975). Dextran produced by *Leuconostoc mesenteroides* NRRL B-512F is a commercial polymer, which has been fermented at a large industrial

*Author for correspondence
E-mail: richard.visser@wur.nl
‡Present address: Unité de Biochimie Physiologique, Institut des Sciences de la Vie, University of Louvain, Croix du Sud 2-20, B-1348 Louvain-la-Neuve, Belgium

scale since 1948 (Groenwall & Ingelman, 1948). It is used in several industrial applications including chromatographic media, soil conditioner (Murphy & Whistler, 1973) and biodegradable hydrogels (Hennink & van Nostrum, 2002). In the latter case, dextran-based gels are used as a delivery system for the specific targeting of drugs to the colon, where they are degraded by a secreted bacterial dextranase. The *L. mesenteroides* NRRL B-512F dextran polymer is water-soluble, and consists of 95% α-(1→6) linkages in the main chain, and 5% α-(1→3)-linked single unit side chains (van Cleve et al., 1956). Its biosynthesis is mediated by dextransucrase DSRS (EC 2.4.1.5), which is a 1527 amino-acid glucosyltransferase (Wilke–Douglas et al., 1989). This enzyme exhibits a high efficiency in bond formation, which makes it a rather attractive polymerase. Its catalytic properties can be summarized as follows: after cleavage of sucrose, a glucosyl residue can be transferred to a growing dextran chain by the so-called two-site insertion mechanism, or to acceptor molecules (Robyt, 1995; Monchois et al., 1999). Glucosylation of acceptor molecules such as maltose and isomaltose are the most effective. Interestingly, it was recently shown that the DSRS glucosylation reaction can also be used for the synthesis of new compounds such as oligosaccharide and surfactant derivatives, giving access to novel industrial applications (Demuth et al., 2002; Richard et al., 2003).

In this study, the production of dextrans, is investigated in a starch-accumulating crop, potato, after expression of *DsrS*. DSRS is targeted to the amyloplast, which has an estimated sucrose concentration of about 10 mM (Farré et al., 2001). In addition, diversification of starch structures might be envisaged with DSRS, because of its high efficiency in glucosylating acceptor molecules, such as maltose, maltodextrins and starch which are present inside the amyloplast (Demuth et al., 2002).

Materials and methods

Construction of binary plant expression vector containing the DsrS gene

An expression cassette containing the patatin promoter (Wenzler et al., 1989), the chloroplastic ferredoxin signal peptide (FD) from *Silene pratensis* (Pilon et al., 1995) fused to the NOS terminator was cloned into the pBluescript SK (pBS SK) plasmid, resulting in pPF. A mature *DsrS* gene from *L. mesenteroides* NRRL B-512F (Wilke–Douglas et al., 1989; U81374) was ligated in frame between the signal peptide and the NOS terminator. The mature *DsrS* gene was amplified by PCR, with a forward primer containing a *Sma*I restriction site (5′-GCCTCATTTGCTC CCGGGACACCAAGT-3′) and a reverse primer containing a *Nru*I restriction site (5′-TGGT GGTTCGCGAGTTATGCTGACACA-3′) using the proofreading *Pfu* turbo DNA polymerase (2.5 units/μl; Stratagene, UK) and cloned into the *Sma*I/*Eco*RV restriction sites of pPF, resulting in pPF*DsrS*. FD and the fused *DsrS* gene were completely sequenced in one direction by Baseclear (The Netherlands) to verify the correctness of the construct. pPF*DsrS* was digested with *Sac*I and *Kpn*I and ligated into a pBIN20 binary vector (Hennegan & Danna, 1998), resulting in pPFS (Figure 1).

Potato transformation

pPFS was transformed into *Agrobacterium tumefaciens* strain LBA 4404 using electroporation

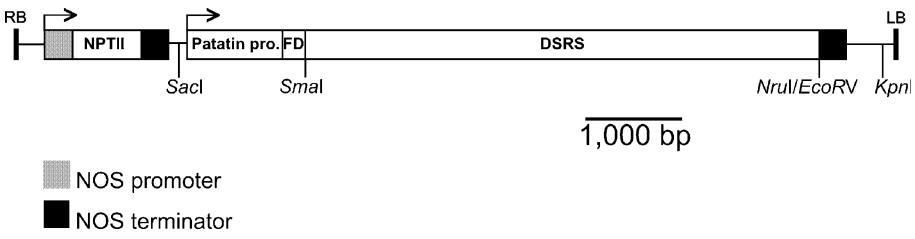

Figure 1. Schematic representation of pPFS binary vector used for potato transformation. The mature *DsrS* gene fused to the FD signal peptide that allowed amyloplastic targeting, was inserted between the highly tuber-expressed patatin promoter and the NOS terminator.

(Takken et al., 2000). Internodal stem segments from two tetraploid potato genotypes (cv. Kardal (KD) and amylose-free (*amf*) mutant (referred to as 1021–91)) were used for *Agrobacterium*-mediated transformation. Transformants were selected on plates with MS30 medium (Murashige & Skoog, 1962) containing kanamycin (100 mg/l). Thirty transgenic, root forming, shoots per genotype were multiplied and five plants of each transgenic line were transferred to the greenhouse for tuber development. The mature tubers were harvested after 18 weeks.

Starch isolation

Potato tubers from the five plants of each transgenic line were combined, peeled and homogenized in a Sanamat Rotor (Spangenberg, The Netherlands). The resulting homogenate was allowed to settle overnight at 4°C and the potato juice was decanted and stored at −20°C for characterization of soluble dextran polymers. The starch pellet was washed three times with water, air-dried at room temperature for at least three days and stored at room temperature.

Immunological detection of dextrans in tuber juices and gelatinized starches

Presence of dextrans was investigated with enzyme-linked immunosorbent assay (ELISA) by using monoclonal anti-α-(1→6) dextran antibodies (45.21.1 (groove-type; IgA/Kappa) and $16.4.12E^{BI}$ (cavity-type; IgA/Kappa)) (Wang et al., 2002). ELISA plates (NUNC, MAXISORP) were coated with 100 µl/well of the groove-type 45.21.1 dextran antibody at a concentration of 5 µg/ml in 1× phosphate-buffered saline solution (PBS). After incubation at 37°C for 120 min, the plates were washed 3 × 5 min with ELISA washing buffer (1× PBS, 0.05% Tween 20^{TM} (v/v) and 0.025% sodium azide (w/v)). The incubations were blocked by adding 200 µl of blocking buffer (1 × PBS, 1% BSA (w/v), 0.05% Tween 20^{TM} (v/v) and 0.025% sodium azide (w/v)) per well for 60 min at 37°C. Subsequently, the plates were washed 3 × 5 min with ELISA washing buffer. 100 µl/well of blocking buffer was added to the appropriate solute (as listed below) which were incubated for 90 min at 37°C.

1. Dextran, referred to as N279 (10 µg/ml), was used for a standard curve and diluted 1:2 in blocking buffer (5; 2.5; 1.25; 0.625 µg/ml).
2. KD-UT potato juice was used for a standard curve in which different concentrations of dextran T40 were added (50; 100; 250; 500; 750; 1000 µg/ml).
3. One ml of potato juice sample was diluted 1:10 in blocking buffer.

Starch samples were used as such and heated at 100°C in a water bath for 20 min before application. After incubation, the plates were washed 3 × 5 min with ELISA washing buffer. 100 µl/well of the cavity-type $16.4.12E^{BI}$ dextran antibody were added at a 1:5000 dilution in blocking buffer. After incubation at 37°C for 60 min, the plates were washed 3 × 5 min with ELISA washing buffer. 100 µl/well of biotin-avidin alkaline phosphatase (AV–AP) were added at a 1:2500 dilution in blocking buffer. After incubation at 37°C for 30 min, the plates were washed 3 × 5 min with ELISA washing buffer. 100 µl/well of substrate solution (1 tablet of alkaline phosphatase substrate/ 8.3 ml diethylamine buffer, pH 9.8) were added. Activities were detected by reading the absorbance at 405 nm.

Expression analysis of DsrS *and starch synthesizing genes using semi-quantitative and real-time quantitative RT-PCR analysis*

RNA was isolated from 3 g (fresh weight) of potato tuber material from selected transgenic lines according to Kuipers et al. (1994).

For semi-quantitative RT-PCR, 50 µg of total RNA was treated with DNAseI and purified using the Gene–elute mammalian total RNA kit (Sigma, The Netherlands). Reverse transcription was performed using 5 µg of total RNA which was incubated for 5 min at 65°C with 500 ng primer polydT (5′-ttttttttttttttttttttttttt-3′) and 12.5 mM of each dNTP in a final volume of 12 µl. After centrifugation (30 sec; 10,000 g), the mixture was incubated for 2 min at 42°C with 4 µl of 5× first-strand buffer (Invitrogen, The Netherlands) and 2 µl of 0.1 M DTT. 1 µl of SuperScript II Rnase H^- reverse transcriptase (200 U/µl; Invitrogen) was added and the mixture was incubated for 50 min at 42°C. Following this, the reaction was terminated by heating the sample for 15 min at

70°C. 2.5 µl of cDNA was used in a standard PCR reaction with the primer/Tm/cycle number combinations as described below. For each combination, the cycle number was optimized in order to remain in the exponential phase of the PCR reaction. *DsrSRT* primers, 5′-CGGTACGGATG CTGAGGACTT-3′ and 5′-GTGTCCGATTAAG TAGTCTAAAGT-3′ (T_m = 59°C, 35 cycles) were based on the *DsrS* gene sequence (Wilke–Douglas et al., 1989). *Ubi3* primers, 5′-GTCAGGCCCAATTACGAAGA-3′ and 5′-AAGTTCCAGCACCGCACTC-3′ (T_m = 55°C, 40 cycles) were used as an internal control and were based on the ubiquitin–ribosomal protein gene sequence (*Ubi3*) from potato (Garbarino & Belknap, 1994; L22576).

Expression levels of *DsrS* and genes involved in starch biosynthesis were also determined in parallel by real-time quantitative RT-PCR and the corresponding primers were designed using the Primer Express software (version 1.5, PE Applied BioSystems, CA, USA): *DsrS* primers, 5′-CAAATCTCAACTGGCGTTCCA-3′ and 5′-GCCGCCCACTCAGTAATCTTT-3′ were based on the same template sequence as that used previously. *SuSy* primers, 5′-GAGGACGTGGCAG GTGAAA-3′ and 5′-GGTACACTGTGTGAC GCCCAT-3′ were based on the sucrose synthase mRNA sequence (Salanoubat & Belliard, 1987; AY205302). *AGPase* primers, 5′-GCTGGGAC CCGACTTTATCC-3′ and 5′-CGGGAATGTC AATCAGACGAT-3′ were based on the ADP-glucose pyrophosphorylase subunit S mRNA sequence (Müller–Röber et al., 1990; X55155). *SSIII* primers, 5′-CACAGGAGGTGTCTGGA AACC-3′ and 5′-TGGAACTTGTGAAGGT-GAGGC-3′ were based on the starch synthase III mRNA sequence (Marshall et al., 1996; X95759). *SBEI* primers, 5′-CCGAGCCCCACGAATC-TAT-3′ and 5′-GGCTCAGAGCTGCTCATGC-3′ were based on the starch branching I enzyme mRNA sequence (Poulsen & Kreiberg, 1993; X69805). *GBSSI* primers, 5′-GAGCTTCT GGCAGTGAACCC-3′ and 5′-GGCAAGTGG AGCGATTTCTTC-3′ were based on the granule-bound starch synthase I gene sequence (van der Leij et al., 1991; X58453). *Ubi3* primers, 5′-TTCCGACACCATCGACAATGT-3′ and 5′-CGACCATCCTCAAGCTGCTT-3′ were used as an internal control as described previously. For real-time quantitative RT-PCR, 1 µg of total RNA was treated with 0.5 µl DNAse I RNAse free (10 U/µl; Invitrogen) and incubated with 5 µl of 10 × Taqman RT buffer, 11 µl of 25 mM $MgCl_2$, 10 µl of 10 mM dNTP mix, 2.5 µl of 50 µM random hexamer primers, 1.0 µl RNAse inhibitor (20 U/µl) and H_2O until a final volume of 39 µl for 30 min at 37°C and 5 min at 75°C. For reverse transcription, the mixture was incubated 10 min at 25°C and 30 min at 48°C with 1 µl of MultiScribe reverse transcriptase (50 U/µl; Applied Biosystems). Following this, the reaction was terminated by heating the sample for 5 min at 95°C. Aliquots of 50 ng of cDNA were used in SYBR-Green PCR according to the manufacturer's protocol on the ABI PRISM7700 sequence detection system (Perkin–Elmer Applied Biosystems) with the primers mentioned above. Relative quantitation of the target RNA expression level was performed using the comparative Ct method according to the User Bulletin # 2 (ABI PRISM7700 sequence detection system, December 1997; Perkin–Elmer Applied Biosystems). The Ct value is defined as the PCR cycle at which the amount of amplified target RNA reaches a fixed threshold. The differences in the Ct values, called ΔCt, between the target RNA and the endogenous *Ubi3* RNA were calculated in order to normalize the differences of cDNA concentrations present in each reaction. The differences in the ΔCt, called ΔΔCt, between a transformed and an non-transformed potato plant were calculated in order to relate the target RNA expression level to that of non-transformed plants. The target RNA expression level of transformed plants was calculated using the equation 2-EXP (ΔΔCt). The relative RNA expression is considered as significant when $-0.5 <$ relative RNA expression > 0.5.

Determination of morphological and physicochemical properties of starch granules

Analysis of starch granule morphology was performed by light microscopy (LM) (Axiophot, Germany) equipped with a Sony color video camera (CCD-Iris/RGB) and scanning electron microscopy (SEM, JEOL 6300F, Japan). For LM, the granules were stained with a 2× diluted Lugol solution before visualization. For SEM, dried starch samples spread on silver tape and mounted on a brass disk were coated with a

20 nm platinum layer. Samples were then examined with a scanning electron microscope operating at an accelerating voltage of 1.5–3.5 keV. The working distance was 9 mm.

Median values of the granule size distribution (d_{50}) were determined with a Coulter Multisizer II, equipped with an orifice tube of 200 μm (Beckman–Coulter, UK). Approximately 10 mg of starch was suspended in 160 ml Isoton II and the granule size distribution was subsequently measured by counting approximately 50,000 granules.

Gelatinization analysis were performed using a differential scanning calorimeter (DSC, Perkin–Elmer Pyris 1, The Netherlands) equipped with a Neslab RTE-140 cooling system. About 10 mg starch was weighed accurately into a stainless-steel pan and water was added until a starch moisture content of 20% was obtained. The pan was sealed and equilibrated overnight at room temperature before DSC analysis. The measurements were performed at a heating rate of 10°C/min from 40°C to 100°C. Before use, the DSC was calibrated with indium and zinc, and an empty pan was used as a reference. The onset temperature of gelatinization (T_0) and the enthalpy (ΔH) were calculated automatically. The reported values are the average of three measurements.

Amylose content was determined as described by Hovenkamp–Hermelink et al. (1988). Starch was diluted in 50 μl $HClO_4$ (35%), followed by determination of the absorption at 618 nm and 550 nm after staining with Lugol solution.

For starch content determination, about 50 mg of potato tuber material was homogenized in 0.5 ml of 8 M HCl (25%). After adding 2 ml of DMSO, the samples were shaken for 1 h at 60°C. Subsequently, 0.8 ml 5 M NaOH and 3.7 ml 0.1 M citric acid buffer pH 4.6 were added. After adjusting the volume to 10 ml with water, the samples were centrifuged for 10 min at 10,000 g. 20 μl of supernatant were used for starch determination using the Boehringer kit (Boehringer, Germany) in a microplate reader (BioRad 3550-UV). Calculations were performed by using glucose release from a known amount of starch as a standard.

For determination of the chain length distribution, 5 mg of (transgenic) starch was suspended in 250 μl of DMSO and gelatinized for 15 min at 100°C. After cooling down to room temperature, 700 μl of 50 mM NaAc buffer pH 4.0 was added. A sufficient amount of isoamylase (Hayashibara Biochemical Laboratories, Japan; 59,000 U/mg protein) to debranch the starch polymers completely was added to the mixture, which was incubated for 2 h at 40°C. After inactivation of the enzyme for 10 min at 100°C, 1 ml of 25% DMSO was added. For high-performance size-exclusion chromatography (HPSEC), 1 ml was used as such. For high-performance anion-exchange chromatography (HPAEC), the sample was diluted 5 times with a 25% DMSO solution. In parallel, undiluted isoamylase-treated samples were incubated with a sufficient amount of porcine pancreas α-amylase (Merck, Germany; 250 U/mg protein) to investigate whether contiguous α-(1→6) glucosyl residues linked to amylopectin side chains were present. After incubation for 3 h at 25°C in 50 mM NaAc buffer pH 6.9 and inactivation of the enzyme for 10 min at 100°C, 1 ml was used for HPAEC analysis.

HPSEC was performed on a P680 HPLC pump system (Dionex, USA) equipped with an ASI-100 automated sample injector (Dionex) and three TSKgel columns in series (a G3000 SWXL and two G2000 SWXL; 300 × 7.5 mm; Montgomeryville, USA) in combination with a TSKgel SWXL guard column (40 × 6 mm) at 35°C. Aliquots of 100 μl were injected and eluted with 10 mM of NaAc buffer (pH 5.0) at a flow rate of 0.35 ml/min. The effluent was monitored using a RID-6A refractometer (Shimatzu, Japan). This system was calibrated with dextran standards (10, 40, 70, 150, 250, 500 kDa; Pharmacia, Sweden). Dionex Chromeleon software version 6.50 SP4 Build 1000 was used for controlling the HPLC system and data processing.

In order to obtain a better separation of the smaller amylopectin side chains (in the range of 2 to 45 glucose residues), HPAEC was performed on a GP40 gradient pump system (Dionex) equipped with a CarboPac PA 100 column (4 × 250 mm; Dionex) at 35°C. The flow rate was 1.0 ml/min and 20 μl sample was injected with a Dionex AS3500 automated sampler. Two eluents were used, eluent A (100 mM NaOH) and eluent B (1 M NaAc in 100 mM NaOH) as follows: 0 → 5 min (100% eluent B; rinsing phase); 5 → 20 min (100% eluent A; conditioning phase); 20 → 25 min (linear gradient 0 to 20% eluent B; 100 to 80% eluent A); 25 → 50 min (linear gradient 20 to 35% eluent B;

80 to 65% eluent A); 50→ 55 min (linear gradient 35 to 50% eluent B; 65 to 50% eluent A); 55→ 60 min (50% eluent B; 50% eluent A). The sample was injected at 20 min. The eluent was monitored by an ED40 electrochemical detector in the pulsed amperometric mode (Dionex).

Results

Screening and selection of transgenic potato plants producing dextran

FD enabling plastidic protein targeting (Gerrits et al., 2001) was fused to the mature *DsrS* gene. The gene fusion was inserted between the patatin promoter (Figure 1) allowing high tuber expression (Wenzler et al., 1989) and the Nos terminator sequence. Except for the presence of two mutations at the FD▲*DsrS* fusion (VTAM↓ATYKVTLITK▲ATP became VTAM↓ATYKVTLIT**P**▲**G**TP, in which ↓ represents the splice site for amyloplast entry and ▲ the gene fusion), the inserts contained no mutations relative to the wild-type sequences (Smeekens et al., 1985; Wilke–Douglas et al., 1989). After *Agrobacterium*-mediated plant transformation, 30 independent transgenic potato clones were obtained for each genotype (Kardal (KD) and the amylose-free (*amf*) mutant). To ensure enough material, five plants of each transgenic clone were grown in the greenhouse for tuberization. Afterwards, the tubers from all plants of each clone were pooled for further characterization. Transformed potato plant series are referred to as KDDxx and *amf*Dxx, in which D represents the *DsrS* gene and xx the clone number. Untransformed genotypes are referred to as KD-UT and *amf*-UT.

Screening for dextran accumulation in the transformants was performed by analyzing tuber juice and gelatinized starches with ELISA by using an anti-α-(1→6) dextran antibody, the cavity-type $16.4.12E^{BI}$ which recognizes the terminal non-reducing end of the polysaccharide (Wang et al., 2002). In the tuber juice of the KDD series, dextran was detected in 9 out of 30 tubers (29%) in a concentration ranging from 0.3 to 1.7 mg g^{-1} FW (Figure 2). Transformants KDD15, KDD4, KDD5 and KDD30 contained the largest amount of dextran, ranging from 1.0 to 1.7 mg g^{-1} FW. As expected, no dextran was detected in KD-UT plants. In the *amf*D series, dextran was detected in 15 out of 27 tubers (56%), but the amount was lower (0.2 to 0.7 mg g^{-1} FW) (Figure 2). No dextran was detected in *amf*-UT plants. Contrary to tuber juice, no dextran was detected in any of the gelatinized KDD and *amf*D starches.

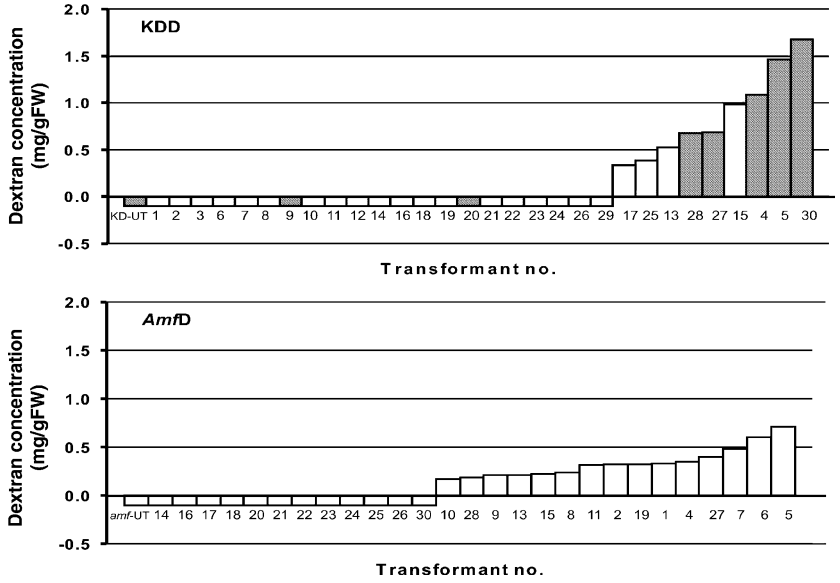

Figure 2. Detection of dextrans accumulated in potato juices by ELISA using anti-dextran antibodies in KDD and *amf*D transformants. Based on the dextran concentration (in mg g^{-1} FW), three categories of transformants were made, where (−), (+) and (++) represent no, intermediate and high dextran accumulation, respectively. Transgenic clones indicated with grey bars were selected for further characterization.

Subsequent experiments were done on the KDD series, because the accumulation of dextrans was the highest in this genotype. Further characterization of the transgenic starches was performed, because previous studies already demonstrated that the production of novel polymers in the amyloplast can have an influence on starch morphology (Gerrits, 2000; Gerrits et al., 2001). Based on the antibody screening, the transformants were divided in three classes: (−), (+) and (++), representing no, intermediate (≤1.0 mg g^{-1} FW) and high (>1.0 mg g^{-1} FW) levels of dextran, respectively. At least, two transformants of each class were selected for further characterization: KDD9 (−), KDD20 (−), KDD27 (+), KDD28 (+), KDD4 (++), KDD5 (++) and KDD30 (++). RNA was isolated from potato tubers and subjected to semi-quantitative RT-PCR (Figure 3(a)) and real-time quantitative RT-PCR analysis (Figure 3(b)). The expression levels were determined for the *DsrS* and *Ubi3* genes, of which the latter was used as a control because of its known constitutive expression (Garbarino and Belknap, 1994). Heterologous *DsrS* gene expression was detected in the expressers KDD27, KDD28, KDD4, KDD5 and KDD30 (Figures 3(a) and (b)). For KDD20, a small amount of *DsrS* mRNA was detected by real-time quantitative RT-PCR that was not detected by semi-quantitative RT-PCR. No *DsrS* mRNA was detected in KDD9 and in the KD-UT plants. In general, results from the semi-quantitative, real-time quantitative RT-PCR and ELISA correlated very well with each other.

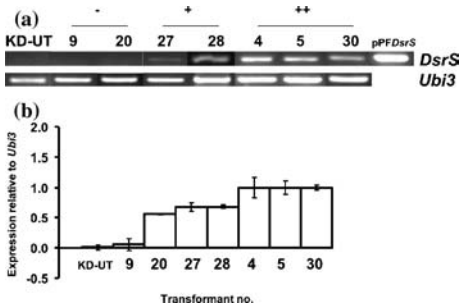

Figure 3. (a) Semi-quantitative RT-PCR analysis of the selected KDD transformants and KD-UT tuber RNA. The upper panel shows the PCR products using the *DsrST* primers that are based on the *DsrS* sequence. The lower panel shows the PCR products using the *Ubi3* primers that served as an internal control. pPF*DsrS*: positive control. (b) Real-time quantitative RT-PCR analysis of the selected KDD transformants and KD-UT tuber RNA. The RNA level of the *DsrS* gene was expressed relative to the amount of *Ubi3* RNA, as described in materials and methods.

Dextran accumulation does not affect plant morphology and tuber growth

The morphology of *DsrS* expressing plants (green parts and tubers) showed no phenotypic alteration in comparison to KD-UT plants (data not shown). For the high expresser KDD30, the tuber number and yield were significantly decreased (about 50%) in comparison to the other selected transformants (data not shown). However, the accumulation of dextran and decreased tuber number and yield are probably not correlated, because the high expressers KDD4 and KDD5 exhibited similar values to the (−) class transformants.

Granule morphology and DsrS *expression are correlated*

Impact of dextran accumulation on starch granule morphology was investigated by LM and SEM. With LM, irregular surfaces (for description, see below) were observed more frequently for the highest expressers (KDD4, KDD5 and KDD30) than for the other selected transformants (data not shown). With SEM, the presence of these irregular surfaces and uncommon forms was confirmed (Figure 4: D-E-F-H-I-J). The granules of these transformants exhibited round-protruded structures in comparison to those of KD-UT, and the granule surface was rough in contrast to that of KD-UT. Altered starch granules, such as those shown in Figure 4 (H, I and J), were scored by analyzing a population of 100 starch granules per selected transformant in triplicate (Figure 5). It can be seen that the percentage of altered starch granules was the highest in the (++) class transformants with KDD30 (16.0 ± 1.0%), followed by KDD5 (11.0 ± 1.0%) and KDD4 (10.3 ± 0.6%). Concerning the (−) and (+) classes transformants (see Figure 4: B–C), the frequency of altered starch granules was much lower, remaining under 7%. From these results, it can be concluded that an altered granule phenotype coincides with dextran accumulation.

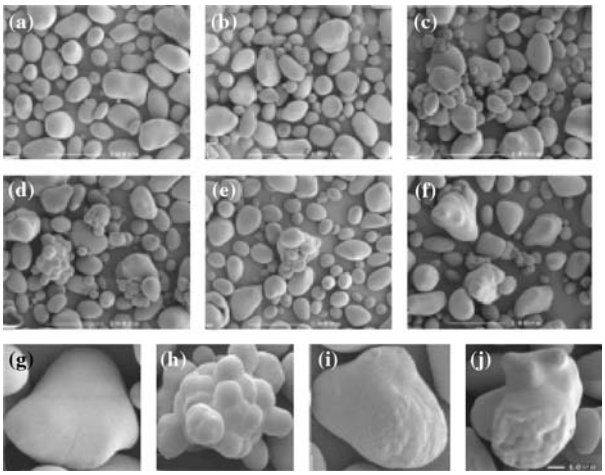

Figure 4. SEM analysis of starch granules (×350) from KD-UT (a) compared to that of selected transformants (KDD9 (b), KDD27 (c), KDD4 (d), KDD5 (e) and KDD30 (f)), and examples of starch granules (×1,000) with altered morphology (KDD4 (h), KDD5 (i) and KDD30 (j)) compared to KD-UT (g).

Dextran accumulation does not interfere with the physicochemical properties of the transgenic starches and the starch content

Median granule size (d_{50}), gelatinization characteristics (T_0 and ΔH), amylose and starch content (Table 1) were determined and no consistent differences were found for the selected transformants compared to KD-UT.

Chain length distributions (HPSEC and HPAEC) (data not shown) were also investigated in order to detect the presence of α-(1→6)-linked dextran chains to starch. After complete debranching of the starch with isoamylase, no differences were observed between the transgenic starches and KD-UT upon HPSEC. Furthermore, after treating the debranched starches with α-amylase, the HPAEC profiles from the transgenic starches were identical to those of KD-UT. These results demonstrate that despite the

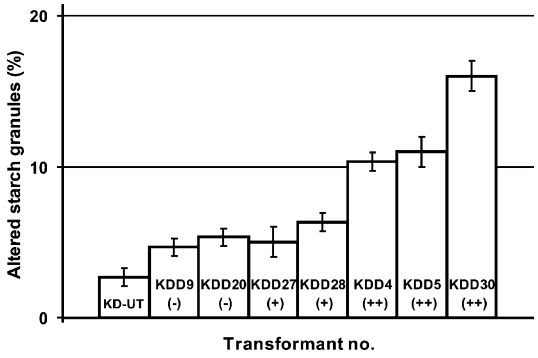

Figure 5. Percentage of granules with altered morphology for the various transgenic starches in comparison with KD-UT.

Table 1. Summary of the physicochemical properties and starch content of the selected transformants and KD-UT

Transformants	d_{50} (μm) [a]	T_0 (°C) [b]	ΔH (kJ/g) [b]	Amylose content (%)	Starch content (mg/g FW)
KD-UT	20.9 (±0.3)	67.0 (±0.5)	14.8 (±0.5)	19.5 (±0.4)	237.2 (±24.8)
DsrS9 (−)	20.9 (±0.6)	67.5 (±0.2)	14.0 (±0.5)	20.4 (±0.1)	245.5 (±21.9)
DsrS20 (−)	22.1 (±0.3)	66.9 (±0.1)	14.1 (±0.9)	20.3 (±0.6)	230.7 (±40.9)
DsrS27 (+)	19.8 (±0.4)	67.7 (±0.2)	14.1 (±0.6)	19.7 (±0.3)	320.7 (±19.6)
DsrS28 (+)	19.0 (±0.5)	66.8 (±0.1)	14.3 (±0.2)	20.7 (±0.2)	257.6 (±34.9)
DsrS4 (++)	18.7 (±0.7)	66.8 (±0.2)	15.1 (±0.4)	20.3 (±0.3)	268.1 (±39.7)
DsrS5 (++)	19.9 (±0.8)	68.3 (±0.3)	14.8 (±0.6)	19.9 (±0.5)	389.4 (±35.7)
DsrS30 (++)	20.6 (±0.4)	66.1 (±0.1)	13.0 (±0.1)	20.1 (±0.2)	314.0 (±38.1)

[a]Median granule size.
[b]Gelatinization characteristics.
Data (±SD) are the average of three independent measurements.

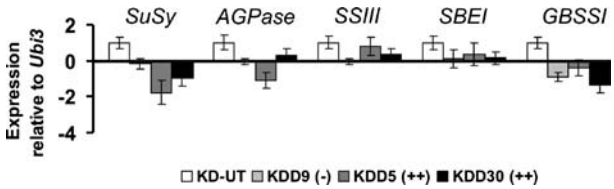

Figure 6. Real-time quantitative RT-PCR analysis of KDD9 (−), KDD5 (+ +) and KDD30 (+ +) transformants and KD-UT tuber RNA. Expression levels of the following genes are indicated: *SuSy*, sucrose synthase; *AGPase*, ADP-glucose pyrophosphorylase subunit S; *SSIII*, starch synthase III; *SBEI*, starch branching enzyme I; *GBSSI*, granule-bound starch synthase I. RNA levels for each gene were expressed relative to the amount of *Ubi3* RNA, as described in materials and methods.

reported high acceptor efficiency of DSRS (Demuth et al., 2002), dextran chains were not covalently attached to starch, but rather present as separate chains. In general, it can be said that despite altered granule morphology, it is obvious that accumulation of dextran does not interfere with the physicochemical properties and starch content of the transgenic starches.

Does dextran accumulation influence the expression level of key genes involved in starch biosynthesis ?

The effect of dextran accumulation on the expression level of genes involved in starch biosynthesis was investigated by real-time quantitative RT-PCR analysis (Figure 6). The following genes were selected: sucrose synthase (*Susy*), ADP-glucose pyrophosphorylase (*AGPase*), starch synthase III (*SSIII*), starch branching I (*SBEI*) and granule-bound starch synthase I (*GBSSI*). They were chosen based on their key role in starch biosynthesis (Kossmann and Lloyd, 2000).

A slight down-regulation in the expression level of *Susy*, *AGPase* and *GBSSI* genes was detected, in particular for the (+ +) class transformant. Despite this, the physicochemical properties and starch content of the transgenic starches were not significantly changed. Concerning the *SSIII* and *SBEI* genes, their expression levels were not affected in comparison to KD-UT.

Discussion

In this study, we describe the production of dextran in potato tubers and its effect on starch biosynthesis, mediated by the expression of the *DsrS* gene from *L. mesenteroides* B-512F. In tuber juice, soluble dextrans were detected with anti-dextran antibodies in both the amylose-containing and amylose-free series, although the Kardal plants accumulated up to 2 times more dextran than the *amf* ones (Figure 2). Absence of granule-bound starch synthase I (GBSSI) in the *amf* background in contrast to the Kardal one, might explain this result. Due to the lack of GBSSI activity, the ADP-glucose pool size in the amyloplast of *amf* mutant plants might be higher in comparison to that of Kardal plants thereby increasing the osmotic potential of this compartment. Consequently, the transport of sucrose from the cytosol into the amyloplast might be hampered, which might result in a lower production of dextrans in the *amf* background.

Heterologous expression of bacterial *DsrS* gene did not interfere with normal plant growth and development. In general, no tuber and starch yield penalties were observed for plants producing dextrans. This could be an advantage for commercialization of dextran production in plant systems. These results were different from those obtained by Gerrits et al. (2001), in which expression of the sucrose-converting levansucrase in the amyloplast triggered severe developmental alterations, even when small amounts of fructan were made.

It was shown that the presence of dextrans could affect granule morphology, which correlated well with the amount of dextran accumulated in the stroma. This result was similar to that obtained by Gerrits et al. (2001) in which fructan production corresponded to altered starch morphology. One explanation for these morphological changes could be a higher viscosity around the granule during its development. Supporting this, *in vitro* studies reported the organization of dextran chains into a network structure that could significantly increase its viscosity (Sidebotham, 1975). Therefore, a more viscous environment around the growing granule

might interfere with its ordered packing of amylopectin side chains, explaining the presence of irregular surfaces.

Direct evidence of dextran accumulation inside starch granules could not be provided by the ELISA and chain length distribution experiments. This result is consistent with the unchanged physicochemical properties of the transgenic starches. Additionally, it demonstrates that despite the reported high acceptor reaction of DSRS (Demuth et al., 2002), this reaction could not be efficiently carried out inside the amyloplast. Expression of *Susy*, *AGPase* and *GBSSI* genes was slightly negatively affected, due to sucrose conversion of DSRS. This might influence the expression level of these genes that are known to be transcriptionally regulated by sucrose (Geigenberger, 2003; Salehuzzaman et al., 1994). *SSIII* and *SBEI* expression levels were not significantly changed, probably because these enzymes are less sensitive to modifications in sucrose supply.

In conclusion, this study is the first report showing that it is possible to produce dextran polymers in potato tubers. Strategies for increasing dextran production could be the targeting of the DSRS enzyme to other subcellular compartments, such as the cytosol or the vacuole, containing higher sucrose concentrations (Farré et al., 2001).

Acknowledgements

The authors would like to thank Isolde Pereira for her assistance with the tissue culture, Dirkjan Huigen for helping with the growth of the plants in the greenhouse, and Ing. Jos Molthoff (PRI-WUR) for his assistance with SYBR-Green analysis.

References

van Cleve JW, Schaefer WC and Rist CE (1956) The structure of NRRL B-512 dextran, by methylation studies. *J Am Chem Soc* **78**: 4435–4438.

Demuth K, Jördening HJ and Buchholz K (2002) Oligosaccharide synthesis by dextransucrase: new unconventional acceptors. *Carbohydr Res* **337**: 1811–1820.

Farré EM, Tiessen A, Roessner U, Geigenberger P, Trethewey RN and Willmitzer L (2001) Analysis of the compartmentation of glycolytic intermediates, nucleotides, sugars, organic acids, amino acids, and sugar alcohols in potato tubers using a nonaqueous fractionation method. *Plant Physiol* **127**: 685–700.

Garbarino JE and Belknap WR (1994) Isolation of a ubiquitin-ribosomal protein gene (*ubi3*) from potato and expression of its promoter in transgenic plants. *Plant Mol Biol* **24**: 119–127.

Geigenberger P (2003) Regulation of sucrose to starch conversion in growing potato tubers. *J Exp Bot* **54**: 457–465.

Gerrits N (2000) Tuber-specific fructan synthesis in potato amyloplasts. Ph.D. Dissertation, Utrecht University, The Netherlands, ISBN 90-393-2345-3.

Gerrits N, Turk SCHJ, van Dun KPM, Hulleman SHD, Visser RGF, Weisbeek PJ et al. (2001) Sucrose metabolism in plastids. *Plant Physiol* **125**: 926–934.

Groenwall AJ and Ingelman BJA (1948) Manufacture of infusion and injection fluids. *US Patent* **2**: 437–518.

Hennegan KP and Danna KJ (1998) pBIN20: an improved binary vector for *Agrobacterium*-mediated transformation. *Plant Mol Biol Rep* **16**: 129–131.

Hennink WE and van Nostrum CF (2002) Novel crosslinking methods to design hydrogels. *Adv Drug Deliv Rev* **54**: 13–36.

Hovenkamp–Hermelink JHM, de Vries JN, Adamse P, Jacobsen E, Witholt B and Feenstra WJ (1988) Rapid estimation of the amylose/amylopectin ratio in small amount of tuber and leaf tissue of the potato. *Potato Res* **31**: 241–246.

Jeanes A, Haynes WC, Wilham CA, Rankin JC, Melvin EH, Austin MJ et al. (1954) Characterization and classification of dextrans from ninety-six strains of bacteria. *J Am Chem Soc* **76**: 5041–5052.

Kok-Jacon GA, Ji Q, Vincken J-P and Visser RGF (2003) Towards a more versatile α-glucan biosynthesis in plants. *J Plant Physiol* **160**: 765–777.

Kossmann J and Lloyd J (2000) Understanding and influencing starch biochemistry. *Critical Rev Plant Sci* **19**: 171–226.

Kuipers AGJ, Jacobsen E and Visser RGF (1994) Formation and deposition of amylose in the potato tuber starch granule are affected by the reduction of granule-bound starch synthase gene expression. *Plant Cell* **6**: 43–52.

van der Leij FR, Visser RGF, Ponstein AS, Jacobsen E and Feenstra WJ (1991) Sequence of the structural gene for granule-bound starch synthase of potato (*Solanum tuberosum* L.) and evidence for a single point deletion in the *amf* allele. *Mol Gen Genet* **228**: 240–248.

Marshall J, Sidebottom C, Debet M, Martin C, Smith AM and Edwards A (1996) Identification of the major starch synthase in the soluble fraction of potato tubers. *Plant Cell* **8**: 1121–1135.

Monchois V, Willemot RM and Monsan P (1999) Glucansucrases: mechanism of action and structure–function relationships. *FEMS Microbiol Rev* **23**: 131–151.

Müller–Röber BT, Kossmann J, Hannah LC, Willmitzer L and Sonnewald U (1990) One of two different ADP-glucose pyrophosphorylase genes from potato responds strongly to elevated levels of sucrose. *Mol Gen Genet* **224**: 136–146.

Murashige T and Skoog F (1962) A revised medium for rapid growth and bioassay with tobacco tissue culture. *Physiol Plant* **15**: 473–497.

Murphy PT and Whistler RL (1973) Dextrans. In: Whistler RL (ed), Industrial Gums (pp. 513–542) Academic Press, New York.

Pilon M, Wienk H, Sips W, de Swaaf M, Talboom I, van 't Hof R, et al. (1995) Functional domains of the ferredoxin transit sequence involved in chloroplast import. *J Biol Chem* **270**: 3882–3893.

Poulsen P and Kreiberg JD (1993) Starch branching enzyme cDNA from *Solanum tuberosum*. *Plant Physiol* **102**: 1053–1054.

Richard G, Morel S, Willemot RM, Monsan P and Remaud-Simeon M (2003) Glucosylation of α-butyl- and α-octyl-d-glucopyranosides by dextransucrase and alternansucrase from *Leuconostoc mesenteroides*. *Carbohydr Res* **338**: 855–864.

Robyt JF (1995) Mechanisms in the glucansucrase synthesis of polysaccharides and oligosaccharides from sucrose. *Adv Carbohydr Chem Biochem* **51**: 133–168.

Salanoubat M and Belliard G (1987) Molecular cloning and sequencing of sucrose synthase cDNA from potato (*Solanum tuberosum* L.): preliminary characterization of sucrose synthase mRNA distribution. *Gene* **60**: 47–56.

Salehuzzaman SNIM, Jacobsen E and Visser RGF (1994) Expression patterns of two starch biosynthetic genes in *in vitro* cultured cassava plants and their induction by sugars. *Plant Sci* **98**: 53–62.

Scheller J, Gührs K-H, Grosse F and Conrad U (2001) Production of spider silk proteins in tobacco and potato. *Nature Biotechnol* **19**: 573–577.

Sidebotham RL (1975) Dextrans. *Adv Carbohydr Chem Biochem* **30**: 371–444.

Smeekens S, van Binsbergen J and Weisbeek P (1985) The plant ferredoxin precursor: nucleotide sequence of a full length cDNA clone. *Nucleic Acids Res* **13**: 3179–3194.

Takken FLW, Luderer R, Gabriëls SHEJ, Westerink N, Lu R, de Wit PJGM et al. (2000) A functional cloning strategy, based on a binary PVX-expression vector, to isolate HR-inducing cDNAs of plant pathogens. *Plant J* **24**: 275–283.

Wang D, Liu S, Trummer BJ, Deng C and Wang A (2002) Carbohydrate microarrays for the recognition of cross-reactive molecular markers of microbes and host cells. *Nature Biotechnol* **20**: 275–281.

Wenzler HC, Mignery A, Fisher LM and Park WD (1989) Analysis of a chimeric class-I patatin-GUS gene in transgenic potato plants: high-level expression in tubers and sucrose-inducible expression in cultured leaf and stem explants. *Plant Mol Biol* **12**: 41–50.

Wilke–Douglas M, Perchorowicz JT, Houck CM and Thomas BR (1989) Methods and compositions for altering physical characteristics of fruit and fruit products PCT patent WO 89/12386.